Bioorganic & Medicinal Chemistry Letters 20 (2010) 2210–2214

Contents lists available at ScienceDirect

Bioorganic & Medicinal Chemistry Letters

journal homepage: www.elsevier.com/locate/bmcl

# Structure-based design of novel human Pin1 inhibitors (II)

Liming Dong, Joseph Marakovits, Xinjun Hou *, Chuangxing Guo *, Samantha Greasley, Eleanor Dagostino, RoseAnn Ferre, M. Catherine Johnson, Eugenia Kraynov, James Thomson, Ved Pathak, Brion W. Murray

*Pfizer Global Research and Development, 10770 Science Center Drive, San Diego, CA 92121, United States*

ARTICLE INFO

*Article history:*
Received 6 November 2009
Revised 8 February 2010
Accepted 8 February 2010
Available online 14 February 2010

*Keywords:*
Pin1
Pin1 inhibitors
Phosphate replacement
PPIase
Anti-cancer agents
SBDD
Carboxylates
Tetrazoles

ABSTRACT

Following the discovery of a novel series of phosphate-containing small molecular Pin1 inhibitors, the drug design strategy shifted to replacement of the phosphate group with an isostere with potential better pharmaceutical properties. The initial loss in potency of carboxylate analogs was likely due to weaker charge–charge interactions in the putative phosphate binding pocket and was subsequently recovered by structure-based optimization of ligand–protein interactions in the proline binding site, leading to the discovery of a sub-micromolar non-phosphate small molecular Pin1 inhibitor.



The peptidyl-prolyl isomerase (PPIase) Pin1 is a potential target for therapeutic intervention and has attracted significant research efforts[1] since its discovery.[2] Pin1 catalyzes the *cis–trans* isomerization of prolyl amide bonds (pSer/Thr-Pro) in its substrate proteins which play critical roles in cell-cycle regulation and are commonly deregulated in human cancer cells.[3] For example, Pin1 is required for proper progression through mitosis[4,5] with depletion of Pin1 causing mitotic arrest and apoptosis in budding yeast and tumor cell lines.[2] Pin1 is up-regulated in wide variety of human tumors and its over-expression correlates with tumor grades and survival.[6] As such, inhibition of Pin1 presents a new opportunity for anti-cancer therapy.[1]

Since Pin1 specifically recognizes a phosphorylated Ser/Thr-Pro peptide motif in its active site,[7] potent Pin1 inhibitors commonly contain a negatively double-charged phosphate group which accounts for a large proportion of binding energy.[8–10] As a phosphate group can be detrimental to cell permeability, discovering whole-cell active Pin1 inhibitors is challenging. We have recently reported a class of novel, potent non-peptide phosphate-containing Pin1 inhibitors.[8] While these high affinity Pin1 inhibitors (e.g., **1a–b**, Fig. 1) provide tools to increase our understanding of the structural elements critical for efficient binding to the Pin1 active site, the presence of a double-charged phosphate moiety[11] is a liability for achieving cell membrane permeability.[12] Recently, moderately potent ($K_i$ μM-range) non-phosphorylated small molecule inhibitors[13–17] as well as prodrugs[18] of phosphate-containing inhibitors have been reported.

Initially, the charge–charge interactions between phosphate inhibitors and the active site appeared to be essential for Pin1 inhibition because an alcohol analog, such as **1c** is inactive in Pin1 enzymatic assay. Therefore, replacement of the phosphate group with less charged functional groups such as a carboxylic acid or acid isosteres is investigated. Carboxylic acid and related tetrazole moieties have been incorporated in many successful drugs in clinic.[19] A simple replacement of the phosphate with either a sulfate or carboxylate group (**2**, Fig. 1)[8] diminishes the affinity to Pin1, presumably due to suboptimal charge–charge interactions. To shift our chemistry effort toward a new chemical space, we decide to revisit a marginally active compound **3a**, which is an

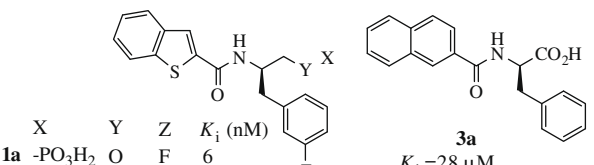


| | X | Y | Z | $K_i$ (nM) |
|---|---|---|---|---|
| **1a** | $-PO_3H_2$ | O | F | 6 |
| **1b** | $-PO_3H_2$ | O | H | 179 |
| **1c** | -H | O | F | inactive |
| **2** | -COOH | $CH_2$ | H | inactive |

**Figure 1.** Simple replacement of the phosphate diminished binding.

* Corresponding authors. Tel.: +1 860 686 0310 (X.H.), +1 858 622 5927 (C.G.).
*E-mail addresses:* xinjun.hou@pfizer.com (X. Hou), alex.guo@pfizer.com (C. Guo).

0960-894X/$ - see front matter © 2010 Elsevier Ltd. All rights reserved.
doi:10.1016/j.bmcl.2010.02.033

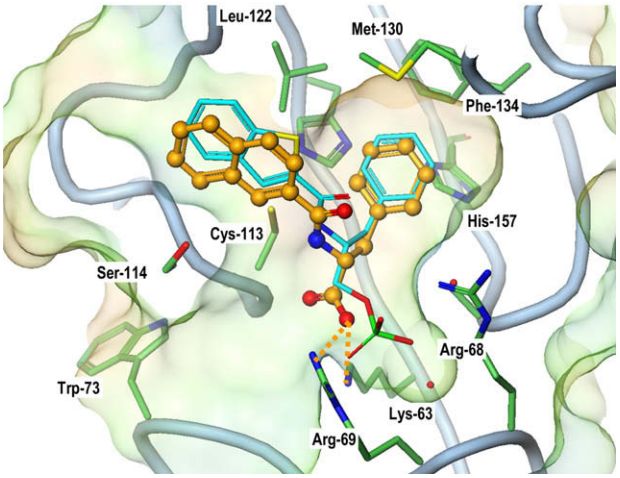


**Figure 2.** A docked model of **3a** (orange) in the X-ray co-crystal structure of **1b** (cyan, Ref. 8) with Pin1 K77Q, K82Q construct.

advanced intermediate of the phosphate inhibitors. Although there is a substantial loss of potency, the binding of compound **3a** to the catalytic site is confirmed by isothermal calorimetric titration and NMR binding studies (data not shown). This observation is surprising because the linker length between the central amido carbon and the negative charged group (the oxygens of the carboxylate) is substantially shorter than that in the phosphate series (**1a** vs **3a**). With the advantage of low MW leads (<350) and good synthetic accessibility, the phenylalanine template is chosen for further optimization.

The model of **3a** (Fig. 2) in the co-crystal structure of **1b** shows a slight shift in the binding of benzyl group, and reveals a gap between the carboxylate and the charge pocket formed by Lys-63, Arg-68, and Arg-69. One of the carboxylate acid oxygens makes a hydrogen bond to Arg-69 and Lys-63 and the other oxygen is unsatisfied. It is evident that the binding of the initial lead (**3a**) may be improved by either introducing substitution(s) to fill the space or inserting a methylene between the amido carbon and the carboxylate so that the phenyl can reach deeper into the proline pocket. Based on this hypothesis, a number of naphthylamido acid analogs are synthesized (Scheme 1)[20] and tested in Pin1 enzymatic assay.[8,20]

As shown in Table 1, benzene substitutions (**R** groups) at the 2-position (**3b–d**) are less active. As expected, small substitutions at the 3-position (e.g., **3f**) increase the potency, reaching the small pocket near Phe-134 and His-157 as previously observed in the non-peptide phosphate Pin1 inhibitors.[8] Surprisingly, larger groups at the 3-position (**3h**, **3j**, **3l** and **3n** vs **3f**) also improve the inhibitory potency—a trend that was not observed in the phosphate series.[8] One hypothesis is that the shorter linker to the acid group in these series pulls the benzyl group away from the bottom of the Pin1 prolyl pocket, creating additional space between Phe-134 and the benzyl group. A bulkier substitution on the phenyl would increase the hydrophobic interaction with the prolyl pocket and allow closer charge–charge interactions with the phosphate recognition site consist of Lys-63, Arg-68, and Arg-69. In order to test this hypothesis, seven β-amino acid analogs (Table 1, linker $n = 1$) are designed and synthesized. The observed SAR is generally in-line with the hypothesis—when substitutions are small (**3f** vs **3g**, **3n** vs **3o**), there are slight improvements in activity of β-amino acids over α-amino acids. But when the substitutions are larger (**3m** vs **3l**, **3q** vs **3p**, and **3v** vs **3u**), β-amino acids are less active, indicating that extending the carboxylate further into the charge pocket is no longer beneficial. The analogs with an '*S*' configuration (not shown) are synthesized and found to be 10–30 times less active than corresponding '*R*' isomers shown here.

**Table 1**
SAR of fragment binding to prolyl pocket

| No. | R | Linker ($n$) | $K_i$ (μM) |
|---|---|---|---|
| **3a** | H | 0 | 28 |
| **3b** | 2-$CF_3$ | 0 | 93 |
| **3c** | 2-F | 0 | 63 |
| **3d** | 2-CN | 0 | 351 |
| **3e** (racemic) | 2,3-di-F | 0 | 103 |
| **3f** | 3-F | 0 | 12 |
| **3g** | 3-F | 1 | 5.7 |
| **3h** | 3-$CH_3$ | 0 | 2.8 |
| **3i** | 3-$CH_3$ | 1 | 9.7 |
| **3j** | 3-CN | 0 | 3.2 |
| **3k** | 3-CN | 1 | 2.3 |
| **3l** | 3-$CF_3$ | 0 | 1.8 |
| **3m** | 3-$CF_3$ | 1 | 13 |
| **3n** | 3-Cl | 0 | 3.4 |
| **3o** | 3-Cl | 1 | 2 |
| **3p** | 3,4-Di-F | 0 | 23 |
| **3q** | 3,4-Di-F | 1 | 82 |
| **3r** | 3,4-Di-Cl | 0 | 2.2 |
| **3s** | 3,4,5-Tri-F | 0 | 9.0 |
| **3t** | 4-CN | 0 | 3.0 |
| **3u** | 4-$CF_3$ | 0 | 11 |
| **3v** | 4-$CF_3$ | 1 | 121 |
| **3w** | 4-$CH_3$ | 0 | 17 |

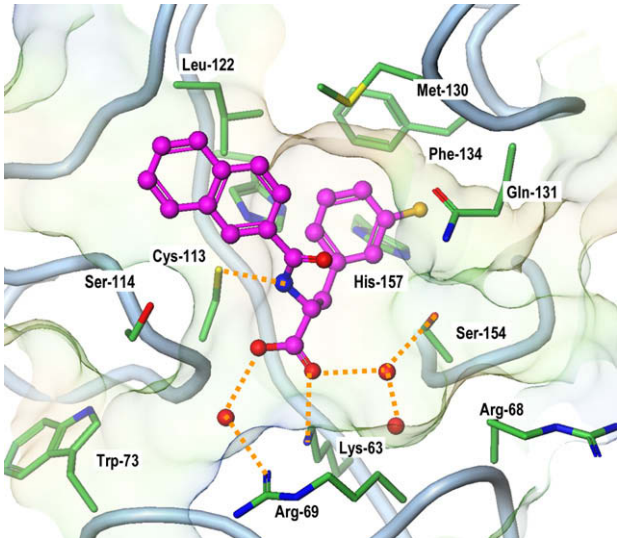


**Figure 3.** X-ray co-crystal structure of **3f** with Pin1 K77Q, K82Q construct (PDB: 3I6C, Ref. 20).

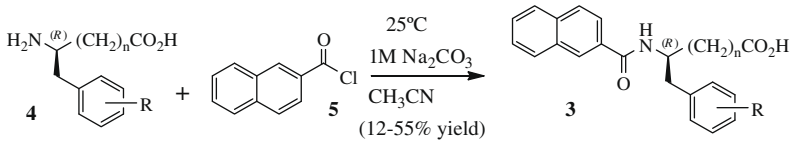


**Scheme 1.** Syntheses of analogs of **3a**.

The co-crystal structure of **3f** with Pin1 (Fig. 3) represents our first Pin1 protein structure with a non-phosphate small molecular inhibitor bound. The co-crystal structure confirms the hypothesis that the carboxylic group does not fully occupy the phosphate pocket.

The binding mode of **3f** is similar to that of the phosphate-containing inhibitors such as **1a–b**,[8] as shown in Figure 3. The 3-fluorophenyl ring occupies the prolyl binding pocket and is in close contact to a hydrophobic region formed by Phe-134, Met-130, and Leu-122 with an edge-on interaction with the His-157 and Phe-134. The fluorine is situated in a small pocket near Phe-134 and His-157. Because of the shorter linker between the charged group and the 3-fluorophenyl ring, the phenyl ring is shifted slightly outward toward the charge pocket in comparison with phosphate inhibitor (Fig. 3), similar to the model in Figure 2. This subtle change in binding conformation of the phenyl ring indicates that there is some degree of elasticity in fitting the phenyl group to the prolyl pocket, consistent with the observed SAR (Table 1). Similar to a non-peptide phosphate inhibitor,[8] the naphthalene ring contacts the hydrophobic surface region near Leu-122. The most significant difference from the binding mode of phosphate-containing inhibitors is the network of charged–charged interactions of the carboxylate. Instead of directly interacting with Arg-68 and Arg-69 side-chains, as observed for phosphate-containing inhibitors, the carboxylate forms a water-mediated interaction with Arg-69 and has no interaction with the disordered Arg-68 side-chain. One carboxylate oxygen makes a good H-bond interaction to a water molecule (2.9 Å) and the other oxygen interacts directly with Lys-63 (2.9 Å). Interestingly, this second carboxylic oxygen also interacts with a crystal water molecule, which bridges the interaction with Ser-154 (3.2 Å) and another buried crystal water molecule in the charged pocket.

While the carboxylate acidic forms a hydrogen bond with Lys-63 on the edge of the basic cluster, it leaves the rest of the phosphate recognition pocket unfilled. With these observations, we generates two strategies to improve potency: (1) replace the carboxylic acid with acid isosteres of different sizes to interact with the charged pocket, and (2) extend the linker between the amido carbon and phenyl group to extend the charge interaction and maintain the dual edge-on interactions with Phe-134 and His-157 in the proline pocket.

To test our first hypothesis, we investigated various acid isosteres, including tetrazoles, acylaminothiazoles, and acylsulfonamides.[21] Tetrazole analogs with an amide at the α-carbon ('α-tetrazoles') are readily synthesized via a three step sequence from the corresponding aminoesters (**6**, Scheme 2) whereas the tetrazoles with an amide at the β-carbon ('β-tetrazoles') are prepared from Boc-protected aminoalcohol (**10**) in five steps.[20] In general, α-tetrazoles show comparable activities with their carboxylic acid counterparts while β-tetrazoles such as **14** are less potent than α-tetrazoles (**9a–c**).

Acylaminothiazoles and acylsulfonamides are known isosteres for carboxylic acids.[22] Acylsulfonamide **16** (Fig. 4) has acidity ($pK_a$ 3.73, ACD LAB) comparable to carboxylic acid whereas acylaminothiazole **15** (Fig. 4) has a $pK_a$ close to 7, which has the potential to be more cell-permeable. Both acylaminothiazole **15** and acylsulfonamide **16** are synthesized readily from the corresponding carboxylic acid **3f**.[20] However, **15** and **16** are found to be weaker binders than the corresponding carboxylic acid (**3f**) likely due to lower acidity (acylaminothiazole **15**) or geometry mis-match for the charge–charge interactions (acyl-sulfonamide **16**).

Tetrazole analogs demonstrate comparable Pin1 inhibitory activity compared to corresponding carboxylic acids. However, since the SAR of Pin1 inhibitory activities of these two series tracks and there is no additional potency gain for tetrazoles, the carboxylic acid series is chosen for further optimization due to better synthetic accessibility.[23]

To test the second hypothesis, the length of the linker between the amido carbon and phenyl ring is investigated to optimize charge interactions while maintaining the dual edge-on interactions with Phe-134 and His-157 in the proline pocket. Accordingly, several analogs with longer linkers (straight-chain alkane, more-rigid alkene, and alkyne) are synthesized.[20] The syntheses of these compounds are shown in Scheme 3. The naphthamide **18** is prepared from propargylglycine **17** in good yield via esterification followed by HATU amide formation. The alkyne (**18)** is then coupled with desired aryl iodide using $Pd(PPh_3)_2Cl_2$ as a catalyst. The resulting intermediate **19** is saponified to give desired carboxylic acid product **21** or alternatively the triple bond can be hydroge-

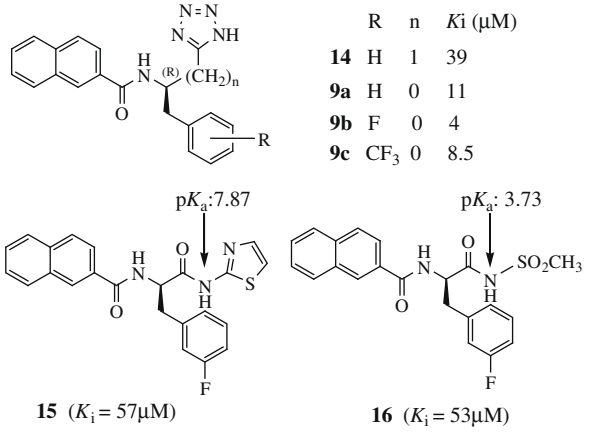


**Figure 4.** Pin1 inhibitors with a carboxylic acid isostere.

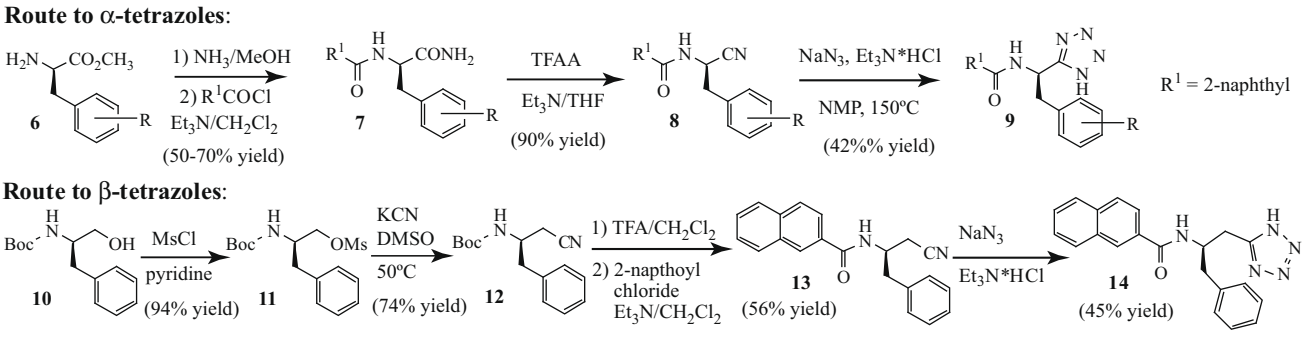


**Scheme 2.** Route to α-tetrazoles.

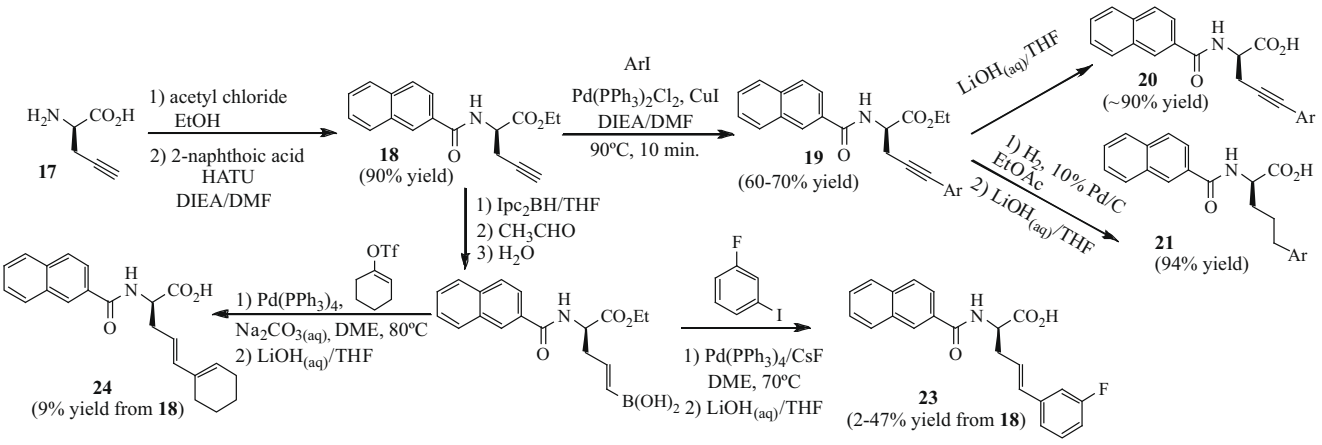


**Scheme 3.**

**Table 2**
SAR of different linker analogs

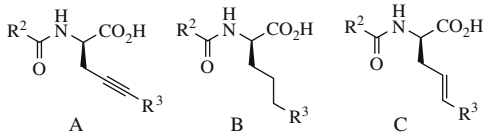


| No. | Core | $R^2$ | $R^3$ | $K_i$ (μM) |
|---|---|---|---|---|
| **20a** | A | 2-Naphthyl | Ph | 12.8 |
| **20b** | A | 2-Naphthyl | 3-F-Ph | 1.87 |
| **20c** | A | 2-Naphthyl | 2-OH-Ph | 4.43 |
| **20d** | A | 2-Naphthyl | 2-thienyl | 7 |
| **21** | B | 2-Naphthyl | 3-F-Ph | 18 |
| **23a** | C | 2-Naphthyl | Ph | 1.8 |
| **23b** | C | 2-Naphthyl | 3-F-Ph | 0.89 |
| **23c** | C | 2-Benzothiophenyl | Ph | 3.7 |
| **24** | C | 2-Naphthyl | Cyclohex-1-enyl | 2 |

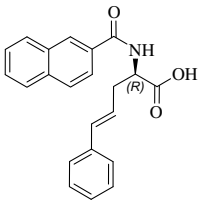

**23a**
MW: 345
LogP: 2.79 (measured)
Solubility: > 347μM
HLM Extraction Ratio: 0.5
Caco $2P_{app}$ ($10^{-6}$cm/sec): AB 2.98; BA 7.73

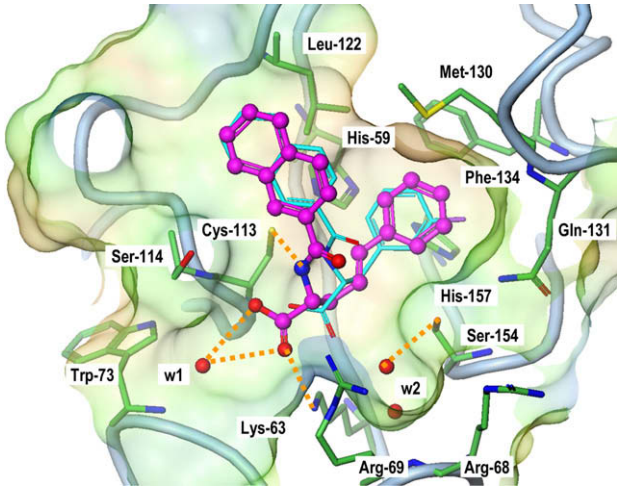


**Figure 5.** X-ray co-crystal structure of **23a** (magenta) with Pin1 K77Q, K82Q construct (distance in A, PDB: 3JYJ, Ref. 20) and its alignment with X-ray structure of **3f** (cyan). The properties of **23a** are shown above.

nated before saponification to the saturated chain (**20**). The alkene analogs (**23–24**) are synthesized by conversion of the terminal alkyne naphthamidoester **18** to the α,β-unsaturated boronic acid **22** which is subsequently subjected to Suzuki coupling and saponification.

All three different linker designs are tested for Pin1 inhibition and the results are summarized in Table 2. There is no gain in potency with an inserted saturated alkyl chain (**21**, $K_i$ = 18 μM), presumably due to the increased flexibility of the molecule that leads to additional entropic penalty. On the other hand, the rigidity offered by the unsaturated linkers increases the binding affinity by an order of magnitude (e.g., **20**, **23**). In general, a fluorine in 3-position of the phenyl ring seems to confer the greatest benefit in binding, and in the case of **23b** it resulted in the first sub-micromolar small molecular non-phosphate Pin1 inhibitor. The binding mode of the styryl analogs (**23a–c** and **24**) is confirmed with a co-crystal protein structure of **23a**, Figure 5. As expected, the binding of **23a** is similar to **3f**, but also extends further into the binding pocket. The phenyl ring moves deeper into the His-157/Phe-134 pocket, and the carboxylate moves slightly outward. The water (w1) molecule mediating interaction between Arg-69 and inhibitor carboxylate (in the structure of **3f**) moves accordingly, but still interacts with the carboxylate at 3.5 Å. This water makes a bidentate interaction to the second carboxylate oxygen. The partially disordered Arg-69 no longer interacts with this water. This may explain the longer interaction distance (3.5 Å) of carboxylate oxygen with the w1 water molecule. Similar to **3f**, the second carboxylate oxygen interacts directly with Lys-63 (2.9 Å), but it no longer interacts with Ser-154 via a water molecule (w2) in the charge pocket.

Selected carboxylate Pin1 inhibitors ($K_i$ <10 μM) are tested in Pin1 whole cell assay, but none of them show any significant binding activity ($IC_{50}$ >50 μM). These carboxylate inhibitors have reasonable cell permeability (e.g., **23a**: CACO2 AB = 2.98, Fig. 5),[24] suggesting on-target potency instead of intrinsic cell permeability may be the under-lined problem. Together with other more desirable ADME properties, such as reasonable metabolic stability (HLM extraction ratio)[25] and excellent solubility, these compounds validated our approach for replacing phosphate with a carboxylate. These studies highlight the need for further improving binding potency to Pin1.

In summary, structure-based design is used to guide the optimization of the phosphate group replacement, leading to the discovery of a series of non-phosphate small molecular Pin1 inhibitors

with low to sub-micromolar inhibitory activity. This study not only confirms the feasibility of replacing the phosphate with a carboxylate for Pin1 binding, but it also highlights the challenge of recovering the loss of binding affinity due to significantly weaker charge–charge interactions. The X-ray co-crystal structures of these small molecular Pin1 inhibitors reveal the flexibility of Pin1 active site interactions on the molecular level as well as a unique binding mode of the carboxylate in Pin1 phosphate recognition pocket. These learnings may be applicable to other related drug targets such as phosphatases or other PPIases.

## Supplementary data

Supplementary data associated with this article can be found, in the online version, at doi:10.1016/j.bmcl.2010.02.033.

## References and notes


1. Recent reviews on Pin1 research: (a) Finn, G.; Lu, K. P. *Curr. Cancer Drug Targets* **2008**, *8*, 223; (b) Lippens, G.; Landrieu, I.; Smet, C. *FEBS J.* **2007**, *274*, 5211; (c) Esnault, S.; Shen, Z. J.; Malter, J. S. *Crit. Rev. Immunol.* **2008**, *28*, 45; (d) Zhang, C. J.; Zhang, Z. H.; Xu, B. L.; Wang, Y. L. *Yao Xue Xue Bao* **2008**, *43*, 9; (e) Xu, G. G.; Etzkorn, F. A. *Drug News Perspect.* **2009**, *22*, 399.
2. Lu, K. P.; Hanes, S. D.; Hunter, T. *Nature* **1996**, *380*, 544.
3. (a) Yeh, E. S.; Means, A. R. *Nat. Rev. Cancer* **2007**, *7*, 381. and references cited therein; (b) Rustighi, A.; Tiberi, L.; Soldano, A.; Napoli, M.; Nuciforo, P.; Rosato, A.; Kaplan, F.; Capobianco, A.; Pece, S.; Di Fiore, P. P.; Del Sal, G. *Nat. Cell Biol.* **2009**, *11*, 133; (c) Zheng, Y.; Xia, Y.; Hawke, D.; Halle, M.; Tremblay, M. L.; Gao, X.; Zhou, X. Z.; Aldape, K.; Cobb, M. H.; Xie, K.; He, J.; Lu, Z. *Mol. Cell.* **2009**, *35*, 11.
4. Lu, K. P. *Prog. Cell Cycle Res.* **2000**, *4*, 83.
5. Winkler, K. E.; Swenson, K. I.; Kornbluth, S.; Means, A. R. *Science* **2000**, *287*, 1644.
6. Lu, K. P.; Wulf, G.; Zhou, X. Z. PCT Int. Appl. WO 2001038878, 2001.
7. (a) Daum, S.; Fanghanel, J.; Wildemann, D.; Schiene-Fischer, C. *Biochemistry* **2006**, *45*, 12125; (b) Pani, E.; Menigatti, M.; Schubert, S.; Hess, D.; Gerrits, B.; Klempnauer, K. H.; Ferrari, S. *Biochim. Biophys. Acta* **2008**, *1783*, 1121.
8. Guo, C.; Hou, X.; Dong, L.; Dagostino, E.; Greasley, S.; Ferre, R. A.; Marakovits, J.; Johnson, M. C.; Matthews, D.; Mroczkowski, B.; Parge, H.; VanArsdale, T.; Popoff, I.; Piraino, J.; Margosiak, S.; Thomson, J.; Los, G.; Murray, B. W. *Bioorg. Med. Chem. Lett.* **2009**, *19*, 5613.
9. Wildemann, D.; Erdmann, F.; Alvarez, B. H.; Stoller, G.; Zhou, X. Z.; Fanghanel, J.; Schutkowski, M.; Lu, K. P.; Fischer, G. *J. Med. Chem.* **2006**, *49*, 2147.
10. Wang, X. J.; Xu, B.; Mullins, A. B.; Neiler, F. K.; Etzkorn, F. A. *J. Am. Chem. Soc.* **2004**, *126*, 15533.
11. At pH 7.4, the phosphoric acid of **1a** likely exists as a double-charged anion. ACD Lab predicted its $pK_{a1}$ = 1.84 and $pK_{a2}$ = 6.34.
12. Pin1 inhibitors with a phosphate group were found to have low permeability in our Caco2 assay [i.e., Papp ($10^{-6}$ cm/s): both A to B and B to A <0.1].
13. Do, Q.-Q. T.; Guo, C.; Humphries, P. S.; Marakovits, J. T.; Dong, L.; Hou, X.; Johnson, M. C. PCT Int. Appl. WO 2006040646, 2006.
14. Bayer, E.; Thutewohl, M.; Christner, C.; Tradler, T.; Osterkamp, F.; Waldmann, H.; Bayer, P. *Chem. Commun. (Cambridge)* **2005**, 516.
15. Daum, S.; Erdmann, F.; Fischer, G.; Feaux de Lacroix, B.; Hessamian-Alinejad, A.; Houben, S.; Frank, W.; Braun, M. *Angew. Chem., Int. Ed.* **2006**, *45*, 7454.
16. Bao, L.; Kimzey, A. PCT Int. Appl. WO 2004093803, 2004.
17. Uchida, T.; Takamiya, M.; Takahashi, M.; Miyashita, H.; Ikeda, H.; Terada, T.; Matsuo, Y.; Shirouzu, M.; Yokoyama, S.; Fujimori, F.; Hunter, T. *Chem. Biol.* **2003**, *10*, 15.
18. Zhao, S.; Etzkorn, F. A. *Bioorg. Med. Chem. Lett.* **2007**, *17*, 6615.
19. Based on retail sells, 26 of the top 200 marketed drugs in year 2008 contain either carboxylic acids or tetrazoles, http://www.chem.cornell.edu/jn96/outreach.html.
20. See Supplementary data.
21. Herr, R. J. *Bioorg. Med. Chem.* **2002**, *10*, 3379.
22. Uehling, D. E.; Donaldson, K. H.; Deaton, D. N.; Hyman, C. E.; Sugg, E. E.; Barrett, D. G.; Hughes, R. G.; Reitter, B.; Adkison, K. K.; Lancaster, M. E.; Lee, F.; Hart, R.; Paulik, M. A.; Sherman, B. W.; True, T.; Cowan, C. *J. Med. Chem.* **2002**, *45*, 567.
23. Hopkins, A. L.; Groom, C. R.; Alex, A. *Drug Discovery Today* **2004**, *9*, 430.
24. Press, B.; Di Grandi, D. *Curr. Drug Metab.* **2008**, *9*, 893. and references cited therein.
25. Lewis, M. L.; Cucurull-Sanchez, L. *J. Comput. Aided Mol. Des.* **2009**, *23*, 97.